Biochimica et Biophysica Acta 1837 (2014) 1955–1963

Contents lists available at ScienceDirect

Biochimica et Biophysica Acta

journal homepage: www.elsevier.com/locate/bbabio

Mass spectrometry footprinting reveals the structural rearrangements of cyanobacterial orange carotenoid protein upon light activation

Haijun Liu [a,b,c,*], Hao Zhang [b,c], Jeremy D. King [a,c], Nathan R. Wolf [c], Mindy Prado [a,c,1], Michael L. Gross [b,c], Robert E. Blankenship [a,b,c]

[a] Department of Biology, Washington University in St. Louis, MO 63130, USA
[b] Department of Chemistry, Washington University in St. Louis, MO 63130, USA
[c] Photosynthetic Antenna Research Center (PARC), Washington University in St. Louis, MO 63130, USA

ARTICLE INFO

Article history:
Received 22 July 2014
Received in revised form 9 September 2014
Accepted 12 September 2014
Available online 22 September 2014

Keywords:
Cyanobacteria
Orange carotenoid protein
Photoactivation
Photoprotection
Phycobilisome
Photosynthesis

ABSTRACT

The orange carotenoid protein (OCP), a member of the family of blue light photoactive proteins, is required for efficient photoprotection in many cyanobacteria. Photoexcitation of the carotenoid in the OCP results in structural changes within the chromophore and the protein to give an active red form of OCP that is required for phycobilisome binding and consequent fluorescence quenching. We characterized the light-dependent structural changes by mass spectrometry-based carboxyl footprinting and found that an α helix in the N-terminal extension of OCP plays a key role in this photoactivation process. Although this helix is located on and associates with the outside of the β-sheet core in the C-terminal domain of OCP in the dark, photoinduced changes in the domain structure disrupt this interaction. We propose that this mechanism couples light-dependent carotenoid conformational changes to global protein conformational dynamics in favor of functional phycobilisome binding, and is an essential part of the OCP photocycle.

1. Introduction

Photosynthesis starts with light energy being absorbed by light-harvesting antenna complexes (LHC) and produces energy-rich organic compounds. If light absorption by LHCs exceeds photochemical conversion capacity, the excess excitation energy can lead to rapid damage, especially caused by reactive oxygen species. All photosynthetic organisms thus need to regulate the light-harvesting process to be compatible with cellular energy requirements, and this is accomplished via multiple protective mechanisms [1]. In plants and green algae, the thermal dissipation of excitation energy occurs at the level of the membrane-bound chlorophyll antenna of Photosystem II, a process called non-photochemical quenching [2,3]. The question of whether or not cyanobacteria, the evolutionary progenitor of the chloroplast, have an equivalent photoprotective mechanism had long been unanswered. Red algae and cyanobacteria use a large antenna complex, called a phycobilisome (PBS) [4–6], to absorb light in the spectral range that is inaccessible for chlorophyll *a* (Chl *a*). The absorbed light energy migrates within the subunits of the PBS and is finally funneled to the photochemical reaction centers (RCs) [7–10]. The action spectrum of PBS fluorescence quenching clearly supports that energy quenching by blue light in cyanobacteria is a process that is independent of state transitions [11] and requires carotenoids, possibly protein-bound, or glycosides [12,13]. A breakthrough on understanding the process of non-photochemical quenching in cyanobacteria was achieved by Kirilovsky's group in 2006 when they demonstrated that genetic deletion of *slr1963*, encoding an orange carotenoid protein (OCP), eliminates such blue-light-induced fluorescence quenching [14]. The OCP strongly interacts with the thylakoids (PBS), acting as both a photoreceptor and a mediator that reduces the amount of absorbed light energy [15–17].

Other research investigations indicated that the cyanobacterial water-soluble OCP is a photoactive protein with a chromophore, a carotenoid 3′-hydroxyechinenone (3′-hECN), bound to the protein [18]. The crystal structure of the OCP, isolated by Krogmann's group from the cyanobacterium *Arthrospira maxima* (*A. maxima*) was determined by Kerfeld et al. [19]. The genetic work combined with this research fostered the concept of non-photochemical quenching in cyanobacteria from a broader perspective. The OCP is currently defined as the first photosensory protein discovered with a carotenoid as the pigment [16]. Structurally, the OCP is composed of two distinct domains spanned by a single 3′-hECN chromophore [19] with the conjugation length effectively extended owing to conformational changes in the protein matrix [20]. Functionally, dark-adapted orange OCP (OCP^O) can be

* Corresponding author at: Washington University in St. Louis, One Brookings Drive, Campus Box 1137, St. Louis, MO 63130, USA. Tel.: +1 314 935 6343.
E-mail address: hliu6@wustl.edu (H. Liu).
[1] Present address: Department of Biological Chemistry and Molecular Pharmacology and Department of Pediatrics, Harvard Medical School, Boston, MA 02115, USA.

http://dx.doi.org/10.1016/j.bbabio.2014.09.004
0005-2728/

converted to an active, red form (OCP^r) that is required for effective binding to PBS and quenching of the excited states of PBS-bound bilins [21,22]. The metastable OCP^r quickly converts back to the inactive OCP^o in the dark. Previous spectroscopic studies demonstrated that both the OCP protein framework and 3′-hECN undergo dramatic conformational changes during this process [15,23–25], indicating the close interactions of the pigment and the OCP protein in its orange form. Using the in vitro reconstitution protocol established by Gwizdala et al. [22] and mass spectrometry-based chemical cross-linking techniques, we found that the active monomeric OCP is located in a cove formed by two APC_{660} trimers in the OCP–PBS complex. Using native mass spectrometry (native MS), we were able to demonstrate that the oligomerization state of OCP changes upon conversion to the red form [26],

The characterization of the conformational changes associated with protein function is a central goal of structural biology. This is particularly true for photoactive proteins that contain a chromophore as their light sensor. The knowledge of the mechanisms by which blue light is sensed by microorganisms and higher plants, and of the physiological responses elicited by the blue light photoreceptors, has grown tremendously during the last two decades [27–29]. The common elements in light-activation pathways and molecular-signal transduction of different proteins include an initial conformational change that is localized next to the chromophore site, distortion of the protein structure in the proximity of the chromophore, and then long-range propagation of this distortion to a region of the protein structure such as the N- and C-terminal helices [30,31].

Even though structural and photoactivation models of the OCP have been proposed [17,19,26,32–34], many questions regarding the mechanistic and protein dynamic details in the OCP photocycle remain. For example, what is the structure of the red, active OCP? Dynamically, how is the structural signal, originating in the 3′-hECN upon the absorption of blue light, transmitted to its proteinaceous binding pocket? How does the binding pocket relay these structurally localized changes to the global surface helical or loop structure to ready the OCP for PBS binding? How does the activated OCP become competent for binding of the fluorescence-recovery protein (FRP), which reverses the quenching activity of the OCP^r? The answers to such questions are difficult for X-ray crystallography because it is usually unable to reveal structural information in flexible, highly dynamic and functionally important regions. Required are mechanistic information about the OCP photocycle and identification of the commonalities of intra-molecular signal-transduction mechanisms in pigment-binding proteins [28].

MS-based proteomic techniques have developed rapidly over the past decade, particularly their sensitivity, mass accuracy, and fast data analysis [35–37]. The advent of residue-level, MS-based footprinting techniques have emerged as a powerful structural biology tool for interrogating functional protein dynamics. 1-ethyl-3-[3-dimethylaminopropyl] carbodiimide hydrochloride (EDC)-triggered glycine ethyl ester hydrochloride (GEE) modification coupled with MS identification has been well documented and recently developed for protein footprinting [38–42]. Briefly, EDC reacts with the carboxyl oxygen of either D/E or C-termini to form an active O-acylisourea intermediate that is easily displaced by the nucleophilic modifying reagent GEE [39]. It should be noted that under these experimental conditions, the EDC-triggered GEE modification reactions dominate EDC-mediated cross-linking reactions [38–40], essentially eliminating formation of lysine (K)-D/E cross-links. The reactivity of the carboxyl group on D/E to EDC and, thus, to GEE modification is proportionally related to the solvent-accessible surface area [43,44] of D/E. Carboxyl groups that are surrounded by hydrophobic amino acids or are buried in the interior (channel or cavity) of a protein undergo less or even no modifications [41]. The analytical approach we employed is one that is typically used in proteomics studies for which quantification of modified and unmodified peptides was accomplished from extracted ion chromatograms (EICs) and integrated areas under relevant peaks. The modification extent of a peptide was computed to be the area under a peak representing the modified peptide divided by the sum of the peak area of all forms of that peptide that could be detected by MS. Readers are encouraged to consult relevant literature for detailed calculation procedures [40–42,45].

Our goal is to employ MS-based approaches to investigate photoactive pigment protein complexes, specifically to probe the OCP conformational rearrangements during its photocycle. We report here that carboxyl-group footprinting with glycine ethyl ester (GEE) labeling can track light-induced OCP protein conformational changes. The results indicate that the OCP C-terminal β-sheet functions as a hub in mediating light-induced chromophore conformational changes and protein global structural rearrangements.

2. Materials and Methods

2.1. Growth of Synechocystis sp PCC 6803 and OCP isolation

The growth and the OCP isolation were described elsewhere [15,26].

2.2. Carboxyl group modification

The OCP protein with OD 1.0 at 495 nm was used for EDC triggered GEE modification in 20 mM MOPS, pH 7.0. The modification reaction was carried out for a time course up to 2 h in either dark or light conditions in the presence of GEE (Sigma, St. Louis, MO) and EDC (Pierce, Rockford, IL), using freshly prepared 1.5 M GEE and 0.5 M EDC stock solutions. The reaction was quenched by adding a 1/10 volume of 1 M Tris–HCl (pH 8.0) followed by desalting and buffer-exchange using a Zeba™ column (Thermo Scientific, Rockford, IL) according to the manufacture's protocol. To obtain OCP^r the isolated protein was illuminated with white light at 1000 μmol photons m^{-2} s^{-1} at room temperature for 5 min. Two light schemes were subsequently used after the modification reagents were added to the OCP^r: "light 1" with a light/dark cycle of 1 min/3 min, "light 2" with constant light, to preserve active, red OCP.

2.3. Absorption spectroscopy

The OCP samples, with and without GEE modification were analyzed on a UV-2510PC Shimadzu UV–Vis spectrophotometer (Kyoto, Japan).

2.4. LC–MS/MS

The GEE-modified OCP samples were precipitated and digested following the previous published method with minor changes [46]. The tryptic peptide samples from in-solution digestion were concentrated and desalted by C8 NuTip (NT3C08, Glygen Corporation, Columbia, MD). The peptide sample was dried by speed vacuum. The dry peptide samples were stored at −20 °C before loading to the auto sampler vials for the LC–MS/MS experiment. The samples were reconstituted with 20 μL water containing 0.1% formic acid (solvent A in HPLC). An aliquot (5 μL) was loaded onto a custom-packed column by Eksigent NanoLC system (Eksigent Technologies, Inc. Livermore, CA). The custom-packed column was made by packing reverse-phase C18 material (Magic C18, 5 μm, 200 Å, Michrom Bioresources, Inc., Auburn, CA) into silica capillary tubing terminated with a custom-pulled tip. The gradient was from 2% to 35% solvent B (acetonitrile, 0.1% formic acid) over 50 min at 260 nL/min. The gradient was followed by a 5 min 95% solvent B wash and a 5 min re-equilibration with 100% solvent A. A PicoView Nanospray Source (PV550, New Objective, Inc., Woburn, MA) and an LTQ FT mass spectrometer (Thermo-Scientific, San Jose, CA) were used in the analysis The nano electro-spray parameters were tuned by direct infusion of an Angiotensin II solution (10 μg/mL, 70% solvent A, 30% solvent B). LC–MS data were acquired in standard data-dependent mode controlled by Xcalibur software. Peptide mass spectra (m/z range: 350–2000) were acquired at high mass resolving power (50,000 for ions of m/z 400). The six most abundant ions were fragmented by CID

(collision-induced dissociation) in the linear ion trap (isolation width, 3 Da; activation time, 35 ms; normalized collision energy, 25%; minimum ion counts, 500).

2.5. Protein footprinting data process

The raw data from LC–MS/MS experiment were converted to mgf and mzXML formats by MM file conversion tools (www.massmatrix.net) [47]. The converted data were searched against the *Synechocystis* sp. PCC 6803 sequence database downloaded from UniProt (www.uniprot.org) by Mascot with GEE modifications specified. The modification extent was calculated by following a previously published protocol [40,42].

3. Results and discussion

We studied OCP conformational changes by determining the time-dependent aspartate (D) and glutamate (E) residue labeling under three conditions: 1) dark, inactive-orange form, 2) intermittent light ("light 1"), active-red form, and 3) constant light ("light 2"), active-red form (Fig. 1). We performed the experiments under physiological conditions by using EDC to initiate GEE labeling [40]. The two OCP^r samples were obtained by illumination with white light for 5 min prior to labeling. The time-dependent labeling affords information regarding the general solvent accessibility of D and E (Fig. 1A). To locate the sites that are modified by GEE, we used trypsin digestion followed by LC–MS/MS analysis. We performed peptide-level D/E time-dependent modification at five reaction times (5, 30, 60, 90, and 120 min) on the two photoactivated OCP^r and one dark-adapted OCP^o sample. During modification, the OCP^o sample was kept in the dark, while "light 1" and "light 2" samples were kept in the red form by exposing them to either a light scheme with a light/dark cycle or constant light.

Absorption spectroscopy analysis demonstrated that OCP samples under "light 1" and "light 2" conditions have an identical red-shifted spectrum, which is characterized by a broad peak at 500–510 nm and a loss of the resolution of the vibronic bands [15]. After each time point, the OCP samples were immediately quenched and transferred to an ice bath (see Fig. 1A for a photograph of the samples before sample precipitation, digestion, and analysis). All the samples modified by GEE under dark conditions did not show significant changes in absorption spectra (i.e., no differences in absorption peaks at 476 and 495 nm (Fig. S1A)), indicating no conformational changes after protein modification (the chromophore absorption spectrum is very sensitive to its chemical environment). This indicates that potential artifacts incurred from this modification technology are minimized [42]. Fig. S1C shows the absorption spectra of OCP^r ("light 2", Fig. S1C) samples after 20 min dark relaxation.

Although there is no significant spectral difference between dark-adapted OCP and the two OCP^r samples when modification was terminated at 5 min, we found with increasing modification time that the UV spectra of OCP^r modified in "light 1" and "light 2" show progressive red shifting, with the vibronic band decreasing (Fig. S1) (note that these are samples after 20 min dark relaxation). It appears that GEE footprinting is able to "lock" some fraction of the OCP in its red form (Fig. S1C). This "locking" phenomenon of the OCP^r is further confirmed by using an increased concentration of GEE and EDC (Fig. 1B); after 20 min of dark relaxation, the absorption spectrum of GEE-modified OCP (under constant light illumination) is basically identical to that of active, OCP^r (Fig. 1B) and reference [15]. GEE specifically modifies carboxyl groups of D/E and the C-terminal group. "Locking" OCP in its red state suggests that those modified D/Es cannot adopt their orange-form conformation, indicating that those modified D/E are actively involved in protein conformational changes during the OCP photoactivation. Our next goal is to identify and compare those amino acids in OCP^o and OCP^r.

Using LC–MS/MS, we identified more than 16 tryptic peptides from all of our samples. All identified peptides, including those with one or two missed cleavage sites cover more than 90% of the OCP sequence. This is better coverage than is typically found with membrane protein complexes, which contain large amounts of hydrophobic transmembrane α helix [41,48]. Although two peptides (97–106, 107–112) of

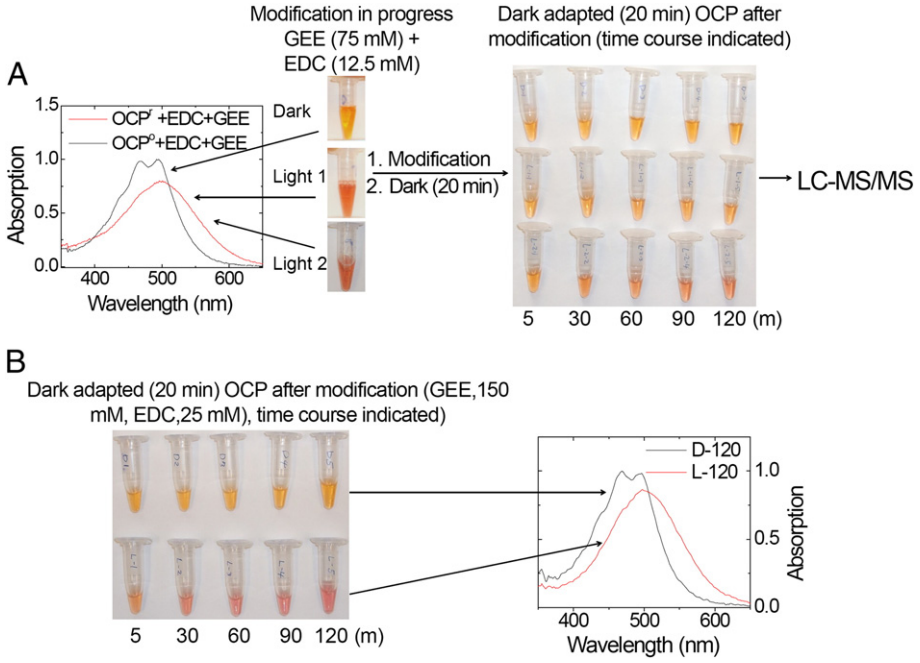

Fig. 1. Experimental design and procedure. Solvent-exposed amino acid residues of the OCP^o and OCP^r were covalently modified by GEE. (A). Chemical modification was performed in the presence of GEE (75 mM) and EDC (12.5 mM). The OCP^r was photoactivated by pre-illumination using white light at intensity of 1000 μmol m^{-2} s^{-1} for 5 min before adding GEE and EDC. The photographs and absorption spectra were taken after 20 min dark adaptation. (B) Modification reactions in the presence of increased concentrations of GEE (150 mM) and EDC (25 mM). Active OCP can be locked in its red form. Photograph was taken after 20 min dark incubation. Absorption spectrum of "locked", OCP^r by GEE modification.

the OCP do not contain any D/E residues, both were identified in our analysis. These two peptides were not used in later data analysis. Incomplete coverage includes some small peptides (2–5 amino acids, AA) resulting from trypsin digestion, which usually elute early and escape detection by LC–MS/MS analysis.

Briefly, according to the modification trend, GEE-modified peptides are classified and listed in three groups (Fig. 2). Modification extents of peptides 2–9, 10–27, 171–185, 255–268, 298–310, 311–317 (group A) of the OCP^r (light 2) show a remarkable difference from those of the corresponding peptides in the OCP^o (Fig. 2A). During the process of mapping all the modification sites in this group, we noticed that they are mostly located in two regions: the interface of the N- and C-terminal domains (E174, E244, D19) and the β-sheet core facing the αA of the N-terminal extension (D6, D19, E258, E261, E262, D304, and E311) (Fig. 2B, C). Time-dependent GEE modification on each site provided more detailed information. For example, the modification level of D6 in peptide 2–9, a peptide fragment in the N-terminal extension of the OCP, does not show a notable difference (0.2%) in the OCP^o and OCP^r when the modification reaction is quenched in 5 min, which is consistent with an absorption spectral analysis (Fig. S1). Although the modification level of D6 increased slowly with time for OCP^o, we found that the modification extent of D6 for OCP^r (light 2) increased much faster than that of D6 in the OCP^o. This behavior must be a consequence of increased reactivity of D6 carboxyl group to GEE labeling in OCP^r. Two light schemes used in this experiment consistently confirmed the metastable nature of OCP^r upon dark relaxation as modification level of the "light 1" is always falls in between dark and ("light 2") (Fig. 2A).

The modification extent difference between dark and light samples results from solvent-accessible surface area changes that reflect the conformational changes between the OCP^o and OCP^r. While in the OCP^r state ("light 1" scheme), the modification trend always falls between that of OCP^o and OCP^r ("light 2" scheme), which are exposed under constant light illumination (Fig. 2A). In contrast, the modification levels of several peptides, 28–49, 70–96, 155–167, 188–234, and 290–297 (group B) increase in all the OCP samples. The protein regions corresponding to these peptides seem to undergo no significant conformational changes upon light activation; however, they are available for modification under all conditions. These sites are mapped onto the OCP structure to show they are mostly located at the far end of both the N- or C-terminal domains (Fig. 2E, F).

Close inspection of GEE modification extents in all the peptide fragments containing D/E indicates that D/E modification extent varies greatly from one site to another; for example, as noted before that D6 modification in peptide 2–9 starts from 0.2% in all the samples and gradually increases to 0.4% and to 1.6% in dark-adapted

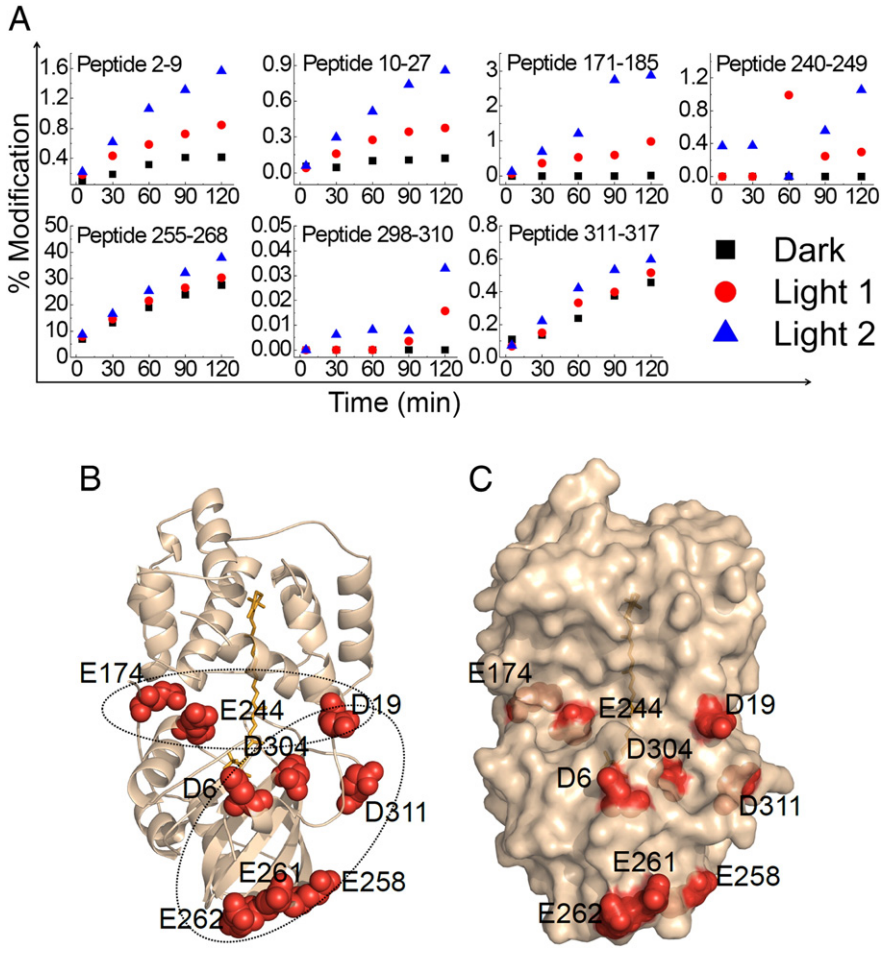

Fig. 2. Modification extents of the OCP and their locations in the OCP structure (PDBID: 3MG1). Two hours time course (5, 30, 60, 90, 120 min). Dark-adapted OCP in a time course modification (black squares), the OCP sample with alternate light (1 min) and dark (3 min) scheme during chemical modification, after an initial, complete photoactivation (5 min), red triangles, and the OCP sample with constant actinic light exposure during the whole process, blue triangles. (A) Polypeptides containing D/E with increased modification upon photoactivation of the OCP. (B) The OCP monomer, cartoon representation with D/E as red spheres. (C) Surface representation of (B). (D) Polypeptides containing D/E showing no modification changes and their locations (D/E as green spheres) in the OCP structure (E, F). (G) Polypeptides containing D/E with decreased modification upon photoactivation and their locations represented as blue spheres (H). (I) Global modifications of the OCP, note the circled area: N- and C- terminal domain interface (upper circle) and αA and its surrounding modified amino acids (lower circle).

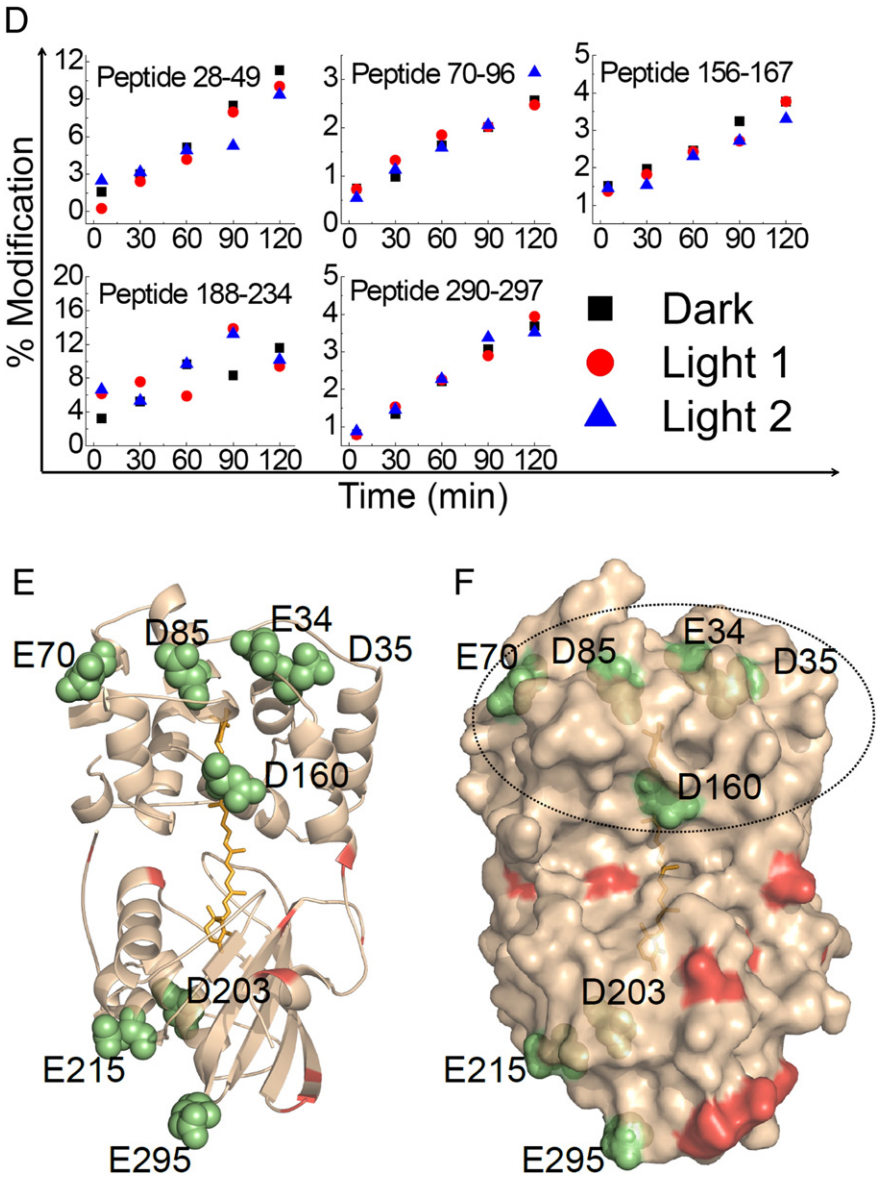

Fig. 2 (*continued*).

and light-activated OCP ("light 2"), respectively. However, E115 and E118 modification levels in peptide 113–155 (Fig. 2G) start at 40% in both OCP^o and light OCP^r ("light 1" and "light 2") and end at 50% and 70% in "dark" and "light 2" samples, respectively. It is likely that some labeling may occur very rapidly in a burst phase, before the first time point (5 min) of our experiment (Fig. 1G). This variation of site-specific modification is related to a reactivity difference of D/E that is a function of solvent-accessibility changes. Although charged amino acids are usually located on the surface or in channels, some microenvironments may completely block the solvent accessibility of these residues. Generally, the modification extent of D/E increases in a time-dependent-manner, even for the OCP^o (Fig. 2A, D, and G). Very interestingly, we do see some D/E sites that underwent no modification increase at all in the OCP^o even at 120 min; examples are D174, E244, and D304 in peptide 171–185, peptide 240–249, and 298–310, respectively (Fig. 2A). Additionally, MS analysis of samples in which increased GEE and EDC were used (Fig. 1B, 120 min sample) also support that these sites undergo extremely low modification in OCP^o (MS data not shown).

Another group of peptides (Group C, Fig. 2G) undergo modification under both "dark" or "light 1" or "light 2", with increasing time, but the modification extent of OCP^r increases at a smaller rate than that of the OCP^o. E65, E115 and E118 are examples, and they are located in two peptides 56–69, 113–155 on the N-terminal domain (Fig. 2H). This domain has been proposed to be involved in the PBS binding [25,26].

Upon light activation, structural rearrangements of OCP^r compared to OCP^o are mostly located at the interface of N- and C-terminal domains and the αA facing the C-terminal domain β-sheet core (Fig. 2I). Based on the significantly different modification extents shown by GEE carboxyl footprinting (Fig. 2A, D, G), we were able to pinpoint conformational rearrangements of OCP at the amino-acid level (Fig. 2I). Although the connection between light-induced 3′-hECN conformational changes and the OCP protein matrix conformational rearrangements was previously proposed [15,17,19,23–26], the details of how photoactivated 3′-hECN propagates its conformational changes to the protein matrix and to the surface of OCP are not known.

In OCP, the N- and C-terminal domains interact through two distinct regions. The first 19 N-terminal amino acids, which contain a short α helix (αA), extend away from the N-terminal domain and interact with the solvent-exposed face of the C-terminal domain β-sheet. Our GEE labeling results show that upon light activation, D6 of αA and

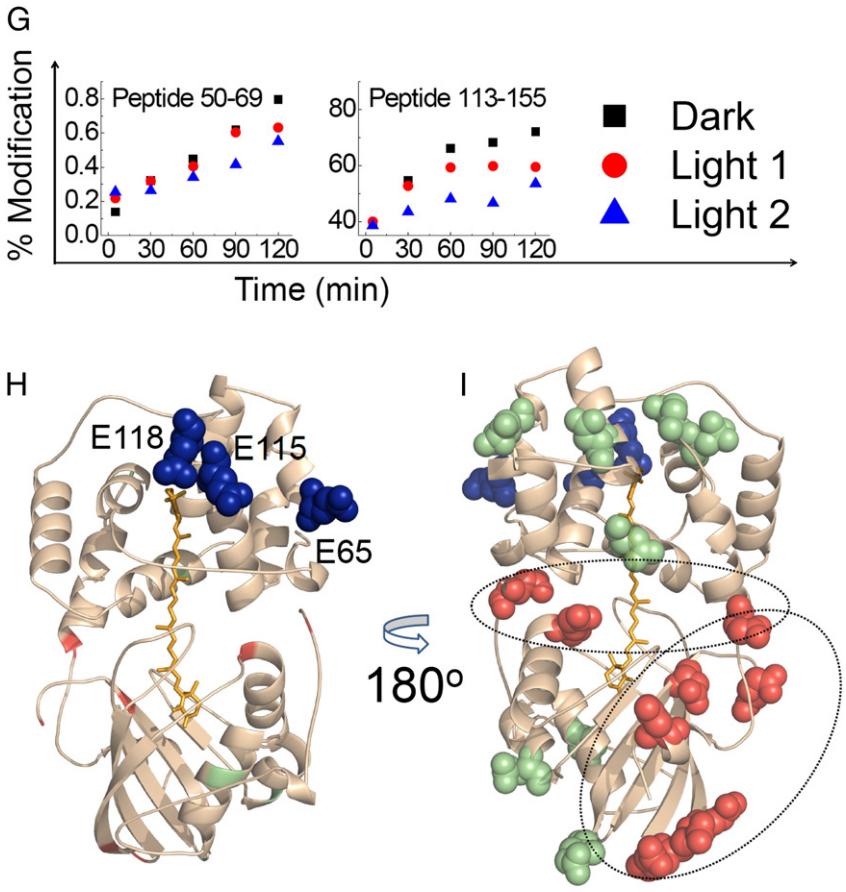

Fig. 2 (*continued*).

D19 of αB undergo large conformational rearrangements (Fig. 2A). The increased modification trend in this region mirrors those of D304 of β5, E311, and E258, E261, E262 (Fig. 2A). The *Synechocystis* OCP structure is very similar to that of *S. maxima* as each contains two molecules in the crystallographic asymmetric unit arranged as an approximate antiparallel dimer [19,32]. Consensus still has not been reached for the OCP oligomerization state. Our previous native MS indicated that upon light activation, a dimer-to-monomer conversion occurs [26]. We, therefore, interpret our current results from the perspective of a light-induced monomerization phenomenon. The dimerization interfaces in all the OCP structures are similar, involving mainly the N-terminal domain [32]. D6 and D19 are located in the interface of the OCP dimer (Fig. 3A), and monomerization of OCP increases the solvent accessibility of these two amino acids, as seen by a resultant increase in chemical modifications. However, the solvent accessibility of both D304 and E311 should not be altered because both residues are located away from the binding interface of the dimeric OCP structure [32] (Fig. 3A). Although the light-induced monomerization hypothesis can explain the increased modification extent of D6 and D19, it fails to explain the observed modification increase of D304, E311, E258, E261, and E262 upon OCP photoactivation; hence the following discussion.

Many amino acids in the interface of the N-terminal extension and the solvent-exposed face of the C-terminal domain β-sheet are conserved [32]. There are six conserved water molecules (Wat1, Wat3, Wat42, Wat76, Wat84, and Wat290) defined by X-ray crystallography [32]. Among these, Wat1, Wat3, and Wat290 are within 3.5 Å of D304 and specifically, Wat1 and Wat290 are 2.8 Å from the carboxyl oxygen of D304 (Fig. 3B), in the range of accepted hydrogen bonding (2.8–3.0 Å). Failure to detect any D304 modification in OCP^o in a 2 h experiment indicates that D304 is not accessible, possibly owing to a shielding effect of the loop area between αA and αB and the conserved structural waters observed in crystals at high resolution [32]. Upon photoactivation, however, modification of D304 of β5 increased significantly, indicating structural rearrangements caused by light absorption of 3′-hECN, which is located opposite the β-sheet core of the C-terminal domain (Fig. 3B). Conserved water molecules play as important a role as conserved amino acids in intramolecular signal transduction, fine-tuning the chemical microenvironment, and regulating activities [51,52]. Displacement of the N-terminal extension from the β-sheet increases solvent accessibility of these structural water molecules and the conserved amino acids on the face of the β-sheet and that of αA where D6 is located (Fig. 3C). The driving force for such movement is unclear at this time.

It was suggested, however, that light absorption by the carotenoid in the OCP increases its effective conjugation length by approximately one double bond so that the pigment in OCP^r adopts a less distorted, more planar conformation than in OCP^o[16]. Subsequent light activation of the carotenoid in the OCP and consequent alternation of the hydrogen bonds between the carotenoid and the C-terminal domain may be propagated to the N-terminal extension through the β-sheet core, which is sandwiched between them (Fig. 3C). A paradigm for this type of intramolecular signal transduction is known for the LOV domain, in which photoactivation of a FAD chromophore alters its hydrogen bonding to the protein matrix, a β-sheet, and triggers the displacement of a short α-helix, Jα, associated with the β-sheet from opposite side, initiating specific biological activity [29,53,54]. In addition to the hydrogen bonds reported previously [25], R289 is hydrogen bonded to D304 (2.9 Å) (Fig. 3B). For OCP, any photochemical changes in the pigment upon light absorption may cause conformational change and alteration of the hydrogen bonds between the carbonyl group of the carotenoid and Y201 and W288. Determining whether R289 mediates the detachment of the N-terminal extension and propagates the light signaling remains unclear and must await further investigation (Fig. 3B, C). E258,

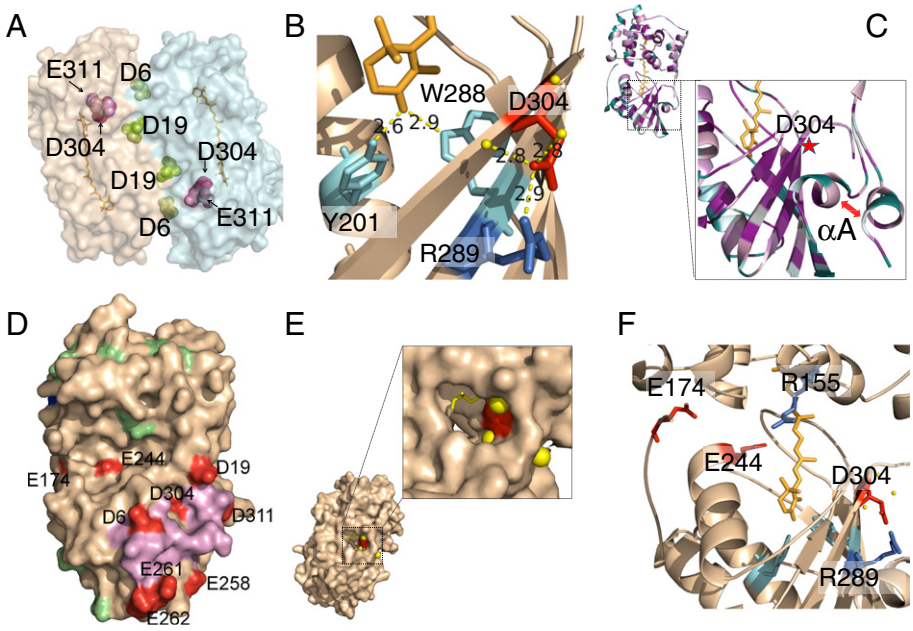

Fig. 3. Structural rearranges of the OCP upon light activation. (A) The OCP dimer structure. D6 and D19 (green) are located in the interface, D304 (magenta) and D311 (pink) are indicated. (B) The microenvironment around D304 (red stick) in β4. The C-terminal domain is in wheat, and the carotenoid is represented by a stick (orange). Y201 and W288, which hydrogen bond to the carbonyl group, are shown as sticks (cyan). R289, which hydrogen bonds to D304, is shown as a stick (blue). Two conserved water molecules are represented as yellow spheres. (C) Highlighting bioinformatics analysis using the ConSurf server [49,50], showing the solvent-exposed face of the C-terminal domain β-sheet and αA. Structurally conserved regions are shown as purple, unconserved regions in teal. The αA helix interacts with the β-sheet domain to lock OCP into an inactive OCP^o, upon illumination, the αA becomes detached and the β-sheet is exposed, loosening the N- and C-terminal interaction, favoring subsequent conformational changes in the interface of N- and C-terminal domain. E304 (red star) is indicated. (D) Surface representation of the OCP. N-terminal extension (pink) is surrounded by D/E (red) showing increased GEE modification. D/E showing no modification changes (lime). (E) E174 (red) is buried in a surface channel with two waters (yellow spheres) hydrogen bonded to it. The glycerol molecule is shown as yellow sticks. (F) Binding pocket of carbonyl group of hECN in the C-terminal domain and the interface of the N- and C-terminal domain. E244, hydrogen bonded to R155, undergoes structural arrangement. E244 is 9 Å from E174. E174 and E244 are shown as red sticks. R155 is represented as a marine stick.

E261, and E262, which undergo increased modification upon OCP photoactivation, are in a region bordering the N-terminal extension (Fig. 3D).

The N- and C-terminal domains of OCP are joined by a 28-amino acid (165–193) link. GEE labeling reveals that E174 of peptide 171–185 in OCP^o displays no increase in modification during the 2 h of labeling (Fig. 2A). This is surprising, partly because the linker loop is thought to be the only region that is structurally flexible and not strongly conserved [19,32]. In our experiment, E174 can be modified only after photoactivation of the OCP (i.e., under "light 1" and "light 2" conditions) but not in its orange form. E174 modification under light conditions also shows time-dependent behavior (Fig. 2A). In the OCP crystal structure, the flexible region consists of the first several residues of the linker (~164–171), which was not resolved owing to large thermal factors [32]. The loop region containing amino acids 172–193 is clearly resolved. Superposition of two molecules in a homodimer (*A. maxima*) indicates that the largest differences between the two molecules are in the loop region defined by residues 163–173 and 179–186 [19], rather than 174–178 ($VAE^{176}PV$) (note that E176 in *A. maxima* is equivalent to E174 in *Synechocystis* 6803). Close inspection of the OCP structure reveals that two conserved water molecules, Wat265 and Wat346, are hydrogen bonded (2.7 and 2.8 Å) to the carboxyl group of E174. A moderately conserved E or D, followed by a highly conserved Pro175 (Pro177 in *A. maxima*), is present in the OCP ortholog. E174 is also in a surface cavity in OCP where one glycerol molecule is present (Fig. 3E). Both oxygen atoms in the carboxyl group of E174 have relatively low *B*-factors (31.22 and 32.85 $Å^2$). As discussed previously, relatively short hydrogen bonding of water to amino acid residues is often functionally important [55,56]. Overall, it seems that the flexible linking loop (165–193) has a moderately conserved (E/D)PVVPP motif in the OCP ortholog [16]. At this time, we do not understand why E174 increases its solvent exposure upon photoactivation.

The central portion of the N- and C- terminal interface is also stabilized by four hydrogen bonds, including two between N104 and W277 and a salt bridge between R155 and E244. N104 and W277 are located in two tryptic peptides, respectively, and they are identified in our MS analysis. However, both peptides contain no D/E, so no GEE footprinting can occur. Our results clearly demonstrate that salt bridging between R155 and E244 in OCP^o completely prevents GEE modification of E244 (Fig. 2A) in 2 h. In contrast, E244 modification increases continuously with time for OCP^r ("light 1" and "light 2", Fig. 2A). This suggests that the salt bridging between R155 and E244 weakens or does not exist for OCP^r, allowing labeling of E244 to occur. Results obtained using genetically modified mutants (R155L, R155E, and E244L-OCP) suggest that in the red form, the salt bridge between R155 and E244 is perturbed [15,25]. Our GEE footprinting data are direct evidence that light illumination causes a salt-bridging alteration of E244–R155. The measured distance between two Cαs of E174 and E244 in the OCP structure (PDBID 3MG1) is ~9 Å. It seems reasonable that conformational rearrangements of one site will affect the other (Fig. 3F).

No D/E site of the N-terminal domain of OCP^r shows increased GEE modification compared to OCP^o (Fig. 2D). The modification extents of E70, D85, D160, D202, and E215 remain constant in both OCP^o and OCP^r (Fig. 2E, F) consistent with the location of these amino acids on the side of OCP that is close to the end of the N-terminal domain (Fig. 2F). We term this the "A side". E65, E115, and E118 undergo less modification in OCP^r compared to OCP^o (the "B side") (Fig. 2G, H). Recently, OCP was proposed to interact with the phycobilisome through its N-terminal domain, specifically via the surface surrounding R155, which is typically buried in the N- and C-terminal interface [25]. Based on chemical cross-linking coupled with MS analysis using a reconstituted OCP^r–PBS complex sample, we were able to confirm that the N-terminal domain is indeed involved in a close association with a site formed by

two allophycocyanin trimers (APC_{660}) in the basal cylinders of the PBS [26]. This is also consistent with a recent report showing that the red carotenoid protein (RCP), which only contains the N-terminal domain and the intact pigment, still retains PBS binding capability and quenches PBS fluorescence [33]. How the N-terminal domain of the OCP structure is rearranged upon light activation to favor efficient PBS binding remains to be determined. We ascribe the driving force of assembling the quenching complex of OCP^r-PBS to be the structural rearrangements on the side where footprinting is reduced (i.e., the "B side", rather than the "A side"), otherwise enabling constitutive binding of OCP^o to PBS. Because the energetic modification of excited-state properties of the bound carotenoid molecule seems less crucial for the quenching properties of the OCP [23,24,57], we hypothesize that it is the physical binding competency of the OCP to PBS upon photoactivation that is required for fluorescence quenching of PBS.

Association of OCP^r to PBS and consequent PBS fluorescence quenching represent two events in the OCP photocycle, while the restoration of normal photosynthetic light-harvesting antenna capacity represents another [58,59]. Our GEE labeling results clearly show that OCP undergoes notable conformational changes upon light activation, so OCP^r must adopt a different conformation than that of OCP^o. It is possible that structural rearrangements of the OCP upon light activation not only prepare OCP for PBS binding but also foreshadow what is to come later in its dissociation from PBS, facilitated by FRP binding, to terminate the quenching state of the OCP^r–PBS complex. The detailed mechanism must await further investigation.

4. Conclusions

Based on previous and our current results, we propose a signal-propagation pathway for OCP activation. Upon illumination of 3′-hECN, its effective conjugation length is increased, enhancing the possibility of breaking the H-bonding network around W288 of β4 (Fig. 3B). Conformational rearrangements of the β-sheet propagate the structural changes to D304 of β5 though R289 of β4, which is hydrogen-bonded to the former, causing the detachment of αA (Fig. 3C). Monomerization may be facilitated by the increased solvent exposure of the β-sheet and of αA. Because the αA helix is one of the two domains through which N- and C-terminal domain interact, disruption of its interaction with the β-sheet would induce subsequent destabilization of the second, central interface, which is stabilized by four hydrogen bonds, including two formed by the pair of residues N104 and W 277 and a salt bridge between R155 and E244. Side B of the N-terminal domain consequently undergoes conformational rearrangements in favor of structural binding of the OCP^r to PBS.

Supplementary data to this article can be found online at http://dx.doi.org/10.1016/j.bbabio.2014.09.004.

Acknowledgments

This research is supported by the Photosynthetic Antenna Research Center, an Energy Frontier Research Center funded by the U.S. Department of Energy (DOE), Office of Basic Energy Sciences (Grant DE-SC 0001035 to R.E.B.), and the National institutes of Health\National Institute of General Medical Sciences (NIGMS Grant 8 P41 GM103422-35 to M.L.G.). H.L., N.R.W. and M.P. were funded by the DOE grant. J.D.K. is supported by a Monsanto Graduate Fellowship. H.Z. was funded equally by the DOE and the NIGMS grants, and instrumentation was made available by both the DOE- and NIH-supported programs.

References

[1] K.K. Niyogi, T.B. Truong, Evolution of flexible non-photochemical quenching mechanisms that regulate light harvesting in oxygenic photosynthesis, Curr. Opin. Plant Biol. 16 (2013) 307–314.
[2] S. de Bianchi, M. Ballottari, L. Dall'Osto, R. Bassi, Regulation of plant light harvesting by thermal dissipation of excess energy, Biochem. Soc. Trans. 38 (2010) 651–660.
[3] A.V. Ruban, M.P. Johnson, C.D. Duffy, The photoprotective molecular switch in the photosystem II antenna, Biochim. Biophys. Acta 1817 (2012) 167–181.
[4] E. Gantt, S.F. Conti, Granules associated with the chloroplast lamellae of *Porphyridium cruentum*, J. Cell Biol. 29 (1966) 423–434.
[5] A.N. Glazer, Light harvesting by phycobilisomes, Annu. Rev. Biophys. Biophys. Chem. 14 (1985) 47–77.
[6] N. Adir, Elucidation of the molecular structures of components of the phycobilisome: reconstructing a giant, Photosynth. Res. 85 (2005) 15–32.
[7] M. Chen, R.E. Blankenship, Expanding the solar spectrum used by photosynthesis, Trends Plant Sci. 16 (2011) 427–431.
[8] C.W. Mullineaux, Phycobilisome-reaction centre interaction in cyanobacteria, Photosynth. Res. 95 (2008) 175–182.
[9] H. Liu, H. Zhang, D.M. Niedzwiedzki, M. Prado, G. He, M.L. Gross, R.E. Blankenship, Phycobilisomes supply excitations to both photosystems in a megacomplex in cyanobacteria, Science 342 (2013) 1104–1107.
[10] A.R. Grossman, M.R. Schaefer, G.G. Chiang, J.L. Collier, The phycobilisome, a light-harvesting complex responsive to environmental conditions, Microbiol. Rev. 57 (1993) 725–749.
[11] K. El Bissati, E. Delphin, N. Murata, A. Etienne, D. Kirilovsky, Photosystem II fluorescence quenching in the cyanobacterium *Synechocystis* PCC 6803: involvement of two different mechanisms, Biochim. Biophys. Acta 1457 (2000) 229–242.
[12] M.G. Rakhimberdieva, I.N. Stadnichuk, I.V. Elanskaya, N.V. Karapetyan, Carotenoid-induced quenching of the phycobilisome fluorescence in photosystem II-deficient mutant of *Synechocystis* sp. FEBS Lett. 574 (2004) 85–88.
[13] M. Scott, C. McCollum, S. Vasil'ev, C. Crozier, G.S. Espie, M. Krol, N.P. Huner, D. Bruce, Mechanism of the down regulation of photosynthesis by blue light in the *Cyanobacterium synechocystis* sp. PCC 6803, Biochemistry 45 (2006) 8952–8958.
[14] A. Wilson, G. Ajlani, J.M. Verbavatz, I. Vass, C.A. Kerfeld, D. Kirilovsky, A soluble carotenoid protein involved in phycobilisome-related energy dissipation in cyanobacteria, Plant Cell 18 (2006) 992–1007.
[15] A. Wilson, C. Punginelli, A. Gall, C. Bonetti, M. Alexandre, J.M. Routaboul, C.A. Kerfeld, R. van Grondelle, B. Robert, J.T. Kennis, D. Kirilovsky, A photoactive carotenoid protein acting as light intensity sensor, Proc. Natl. Acad. Sci. U. S. A. 105 (2008) 12075–12080.
[16] D. Kirilovsky, C.A. Kerfeld, The Orange Carotenoid Protein: a blue-green light photoactive protein, Photochem. Photobiol. Sci. 12 (2013) 1135–1143.
[17] M.Y. Gorbunov, F.I. Kuzminov, V.V. Fadeev, J.D. Kim, P.G. Falkowski, A kinetic model of non-photochemical quenching in cyanobacteria, Biochim. Biophys. Acta 1807 (2011) 1591–1599.
[18] T.K. Holt, D.W. Krogmann, A carotenoid-protein from cyanobacteria, Biochim. Biophys. Acta 637 (1981) 408–414.
[19] C.A. Kerfeld, M.R. Sawaya, V. Brahmandam, D. Cascio, K.K. Ho, C.C. Trevithick-Sutton, D.W. Krogmann, T.O. Yeates, The crystal structure of a cyanobacterial water-soluble carotenoid binding protein, Structure 11 (2003) 55–65.
[20] T. Polivka, C.A. Kerfeld, T. Pascher, V. Sundstrom, Spectroscopic properties of the carotenoid 3′-hydroxyechinenone in the Orange Carotenoid Protein from the cyanobacterium *Arthrospira maxima*, Biochemistry 44 (2005) 3994–4003.
[21] L. Tian, M. Gwizdala, I.H. van Stokkum, R.B. Koehorst, D. Kirilovsky, H. van Amerongen, Picosecond kinetics of light harvesting and photoprotective quenching in wild-type and mutant phycobilisomes isolated from the cyanobacterium *Synechocystis* PCC 6803, Biophys. J. 102 (2012) 1692–1700.
[22] M. Gwizdala, A. Wilson, D. Kirilovsky, In vitro reconstitution of the cyanobacterial photoprotective mechanism mediated by the Orange Carotenoid Protein in *Synechocystis* PCC 6803, Plant Cell 23 (2011) 2631–2643.
[23] T. Polivka, P. Chabera, C.A. Kerfeld, Carotenoid-protein interaction alters the S(1) energy of hydroxyechinenone in the Orange Carotenoid Protein, Biochim. Biophys. Acta 1827 (2013) 248–254.
[24] R. Berera, M. Gwizdala, I.H. van Stokkum, D. Kirilovsky, R. van Grondelle, Excited states of the inactive and active forms of the orange carotenoid protein, J. Phys. Chem. B 117 (2013) 9121–9128.
[25] A. Wilson, M. Gwizdala, A. Mezzetti, M. Alexandre, C.A. Kerfeld, D. Kirilovsky, The essential role of the N-terminal domain of the orange carotenoid protein in cyanobacterial photoprotection: importance of a positive charge for phycobilisome binding, Plant Cell 24 (2012) 1972–1983.
[26] H. Zhang, H. Liu, D.M. Niedzwiedzki, M. Prado, J. Jiang, M.L. Gross, R.E. Blankenship, Molecular mechanism of photoactivation and structural location of the cyanobacterial orange carotenoid protein, Biochemistry 53 (2014) 13–19.
[27] J.M. Christie, Phototropin blue-light receptors, Annu. Rev. Plant Biol. 58 (2007) 21–45.
[28] A. Losi, W. Gartner, Old chromophores, new photoactivation paradigms, trendy applications: flavins in blue light-sensing photoreceptors, Photochem. Photobiol. 87 (2011) 491–510.
[29] S.M. Harper, L.C. Neil, K.H. Gardner, Structural basis of a phototropin light switch, Science 301 (2003) 1541–1544.
[30] S. Rajagopal, S. Anderson, V. Srajer, M. Schmidt, R. Pahl, K. Moffat, A structural pathway for signaling in the E46Q mutant of photoactive yellow protein, Structure 13 (2005) 55–63.
[31] J.R. Cherry, D. Hondred, J.M. Walker, R.D. Vierstra, Phytochrome requires the 6-kDa N-terminal domain for full biological activity, Proc. Natl. Acad. Sci. U. S. A. 89 (1992) 5039–5043.
[32] A. Wilson, J.N. Kinney, P.H. Zwart, C. Punginelli, S. D'Haene, F. Perreau, M.G. Klein, D. Kirilovsky, C.A. Kerfeld, Structural determinants underlying photoprotection in the photoactive orange carotenoid protein of cyanobacteria, J. Biol. Chem. 285 (2010) 18364–18375.

[33] R.L. Leverenz, D. Jallet, M.D. Li, R.A. Mathies, D. Kirilovsky, C.A. Kerfeld, Structural and functional modularity of the orange carotenoid protein: distinct roles for the N- and C-terminal domains in cyanobacterial photoprotection, Plant Cell 26 (2014) 426–437.
[34] F.I. Kuzminov, N.V. Karapetyan, M.G. Rakhimberdieva, I.V. Elanskaya, M.Y. Gorbunov, V.V. Fadeev, Investigation of OCP-triggered dissipation of excitation energy in PSI/PSII-less *Synechocystis* sp. PCC 6803 mutant using non-linear laser fluorimetry, Biochim. Biophys. Acta 1817 (2012) 1012–1021.
[35] R. Aebersold, M. Mann, Mass spectrometry-based proteomics, Nature 422 (2003) 198–207.
[36] E.I. Chen, D. Cociorva, J.L. Norris, J.R. Yates III, Optimization of mass spectrometry-compatible surfactants for shotgun proteomics, J. Proteome Res. 6 (2007) 2529–2538.
[37] A.J. Heck, J. Krijgsveld, Mass spectrometry-based quantitative proteomics, Expert Rev. Proteomics 1 (2004) 317–326.
[38] H. Swaisgood, M. Natake, Effect of carboxyl group modification on some of the enzymatic properties of L-glutamate dehydrogenase, J. Biochem. 74 (1973) 77–86.
[39] D.G. Hoare, D.E. Koshland Jr., A method for the quantitative modification and estimation of carboxylic acid groups in proteins, J. Biol. Chem. 242 (1967) 2447–2453.
[40] J. Wen, H. Zhang, M.L. Gross, R.E. Blankenship, Membrane orientation of the FMO antenna protein from *Chlorobaculum tepidum* as determined by mass spectrometry-based footprinting, Proc. Natl. Acad. Sci. U. S. A. 106 (2009) 6134–6139.
[41] H. Liu, J. Chen, Y.-C. Richard, Huang, D. Weisz, M.L. Gross, H.B. Pakrasi, Mass spectrometry-based footprinting reveals structural dynamics of loop E of the chlorophyll-binding protein CP43 during photosystem II assembly in the cyanobacterium *Synechocystis* 6803, J. Biol. Chem. 288 (2013) 14212–14220.
[42] H. Zhang, Jianzhong Wen, Richard, Y.-C. Huang, R.E. Blankenship, M.L. Gross, Mass spectrometry-based carboxyl footprinting of proteins: method evaluation, Int. J. Mass Spectrom. 312 (2012) 78–86.
[43] M.L. Connolly, Solvent-accessible surfaces of proteins and nucleic acids, Science 221 (1983) 709–713.
[44] T.J. Richmond, Solvent accessible surface area and excluded volume in proteins. Analytical equations for overlapping spheres and implications for the hydrophobic effect, J. Mol. Biol. 178 (1984) 63–89.
[45] H. Zhang, W. Shen, D. Rempel, J. Monsey, I. Vidavsky, M.L. Gross, R. Bose, Carboxyl-group footprinting maps the dimerization interface and phosphorylation-induced conformational changes of a membrane-associated tyrosine kinase, Mol. Cell. Proteomics 10 (2011) (M110 005678).
[46] H. Zhang, R.Y. Huang, P.R. Jalili, J.W. Irungu, G.R. Nicol, K.B. Ray, H.W. Rohrs, M.L. Gross, Improved mass spectrometric characterization of protein glycosylation reveals unusual glycosylation of maize-derived bovine trypsin, Anal. Chem. 82 (2010) 10095–10101.
[47] H. Xu, M.A. Freitas, MassMatrix: a database search program for rapid characterization of proteins and peptides from tandem mass spectrometry data, Proteomics 9 (2009) 1548–1555.
[48] L.K. Frankel, L. Sallans, P.A. Limbach, T.M. Bricker, Identification of oxidized amino acid residues in the vicinity of the Mn(4)CaO(5) cluster of photosystem II: implications for the identification of oxygen channels within the photosystem, Biochemistry 51 (2012) 6371–6377.
[49] O. Goldenberg, E. Erez, G. Nimrod, N. Ben-Tal, The ConSurf-DB: pre-calculated evolutionary conservation profiles of protein structures, Nucleic Acids Res. 37 (2009) D323–D327.
[50] M. Landau, I. Mayrose, Y. Rosenberg, F. Glaser, E. Martz, T. Pupko, N. Ben-Tal, ConSurf 2005: the projection of evolutionary conservation scores of residues on protein structures, Nucleic Acids Res. 33 (2005) W299–W302.
[51] T.E. Angel, M.R. Chance, K. Palczewski, Conserved waters mediate structural and functional activation of family A (rhodopsin-like) G protein-coupled receptors, Proc. Natl. Acad. Sci. U. S. A. 106 (2009) 8555–8560.
[52] T.E. Angel, S. Gupta, B. Jastrzebska, K. Palczewski, M.R. Chance, Structural waters define a functional channel mediating activation of the GPCR, rhodopsin, Proc. Natl. Acad. Sci. U. S. A. 106 (2009) 14367–14372.
[53] T. Koyama, T. Iwata, A. Yamamoto, Y. Sato, D. Matsuoka, S. Tokutomi, H. Kandori, Different role of the Jalpha helix in the light-induced activation of the LOV2 domains in various phototropins, Biochemistry 48 (2009) 7621–7628.
[54] S.M. Harper, L.C. Neil, I.J. Day, P.J. Hore, K.H. Gardner, Conformational changes in a photosensory LOV domain monitored by time-resolved NMR spectroscopy, J. Am. Chem. Soc. 126 (2004) 3390–3391.
[55] S. Rajagopal, S. Vishveshwara, Short hydrogen bonds in proteins, FEBS J. 272 (2005) 1819–1832.
[56] W.W. Cleland, Low-barrier hydrogen bonds and enzymatic catalysis, Arch. Biochem. Biophys. 382 (2000) 1–5.
[57] D.M. Niedzwiedzki, H. Liu, R.E. Blankenship, Excited state properties of 3′-hydroxyechinenone in solvents and in the orange carotenoid protein from *Synechocystis* sp. PCC 6803, J. Phys. Chem. B 118 (2014) 6141–6149.
[58] M. Sutter, A. Wilson, R.L. Leverenz, R. Lopez-Igual, A. Thurotte, A.E. Salmeen, D. Kirilovsky, C.A. Kerfeld, Crystal structure of the FRP and identification of the active site for modulation of OCP-mediated photoprotection in cyanobacteria, Proc. Natl. Acad. Sci. U. S. A. 110 (2013) 10022–10027.
[59] D. Kirilovsky, Modulating energy arriving at photochemical reaction centers: orange carotenoid protein-related photoprotection and state transitions, Photosynth. Res. (2014), http://dx.doi.org/10.1007/s11120-014-0031-7.